Bioorganic Chemistry 110 (2021) 104790

Contents lists available at ScienceDirect

Bioorganic Chemistry

journal homepage: www.elsevier.com/locate/bioorg

Synthesis of new α-Aryl-α-tetralones and α-Fluoro-α-aryl-α-tetralones, preliminary antiproliferative evaluation on drug resistant cell lines and *in silico* prediction of ADMETox properties

Luana G. de Souza [a], Eduardo J. Salustiano [b,*], Kelli M. da Costa [b], Angela T. Costa [c], Vivian M. Rumjanek [c], Jorge L.O. Domingos [d], Magdalena N. Rennó [e], Paulo R.R. Costa [a,*]

[a] *Laboratório de Química Bioorgânica, Instituto de Pesquisa de Produtos Naturais, Universidade Federal do Rio de Janeiro, Ilha do Fundão, CCS, Bloco H - Sala H27, 21941-902 Rio de Janeiro, RJ, Brazil*

[b] *Laboratório de Glicobiologia, Instituto de Biofísica Carlos Chagas Filho, Centro de Ciências da Saúde, Bloco C sala C1-042, Universidade Federal do Rio de Janeiro, RJ 21941-590, Brazil*

[c] *Laboratório de Imunologia Tumoral, Instituto de Bioquímica Médica Leopoldo de Meis, Centro de Ciências da Saúde, Bloco H sala 003, Universidade Federal do Rio de Janeiro, RJ 21941-590, Brazil*

[d] *Departamento de Química Orgânica, Centro de Tecnologia e Ciências, Universidade do Estado do Rio de Janeiro, Rua São Francisco Xavier 524, Pav. Haroldo Lisboa da Cunha – s 406 – Maracanã, 20550-900 Rio de Janeiro, RJ, Brazil*

[e] *Laboratório Integrado de Biologia Computacional e Pesquisa em Ciências Farmacêuticas, Instituto de Biodiversidade e Sustentabilidade (NUPEM), Universidade Federal do Rio de Janeiro, Rua São José do Barreto 764, 27965-045 Macaé, RJ, Brazil*

ARTICLE INFO

Keywords:
Carba-isoflavonoids
α-Tetralone
Molecular descriptors
SAR
Multifactorial drug resistance
ABC transporters
Synthetic lethality

ABSTRACT

α-aryl-α-tetralones and α-fluoro-α-aryl-α-tetralones derivatives were synthesized by palladium catalyzed α-arylation reaction of α-tetralones and α-fluoro-α-tetralones, with bromoarenes in moderate to good yields. These compounds were evaluated for their *in vitro* anti-proliferative effects against human breast cancer and leukemia cell lines with diverse profiles of drug resistance. The most promising compounds, **3b**, **3c**, **8a** and **8c**, were effective on both neoplastic models. **3b** and **8a** induced higher toxicity on multidrug resistant cells and were able to avoid efflux by ABCB1 and ABCC1 transporters. Theoretical calculations of the physicochemical descriptors to predict ADMETox properties were favorable concerning Lipinski's rule of five, results that reflected on the low effects on non-tumor cells. Therefore, these compounds showed great potential for development of pharmaceutical agents against therapy refractory cancers.

1. Introduction

Cancer is a pathological condition where a series of enabling characteristics such as replicative immortality and resistance to cell death grant cells abnormal growth and invasion of healthy tissues and organs [1]. It is a serious public health problem in many parts of the world and considered one of the leading causes of death [2]. The main cause for this disease is the environmental exposure to chemical, physical and biological carcinogenic agents, and evidences indicate that age increase positively correlates to emergence of this disease [3–5]. In addition, the resistance developed by neoplastic cells may hamper the efficacy of chemotherapy-based treatments [6].

Isoflavanones are a sub-group of isoflavonoids comprising interesting biologically active compounds [7,8]. Some synthetic isoflavanones were synthesized by Ma and coworkers [9,10] and evaluated for inhibition of aromatase activity, an enzyme that catalyzes estrogen biosynthesis from androgen precursors. In Fig. 1 are shown compounds **1** and **2** which showed the best inhibitory activity [9,10]. Compound **2** also presented antiproliferative effect on MCF-7 cell line [10]. They are interesting prototypes for the discovery of new antiproliferative agents, in special for pharmaceutical agents against therapy refractory cancers.

In this paper we report the synthesis and the evaluation of the antiproliferative activity of α-aryl-α-tetralones **3**–**12** on drug resistant cell lines.

Compounds **3**–**12** can be considered as isosteres of **1** and **2** in which the oxygen atom at the chromanone ring is replaced by a methylene group. This approach was successfully used by Miller and co-workers

* Corresponding authors.
E-mail addresses: salustiano@bioqmed.ufrj.br (E.J. Salustiano), prrcosta2011@gmail.com (P.R.R. Costa).

https://doi.org/10.1016/j.bioorg.2021.104790
Received 17 July 2020; Received in revised form 5 February 2021; Accepted 28 February 2021
Available online 4 March 2021

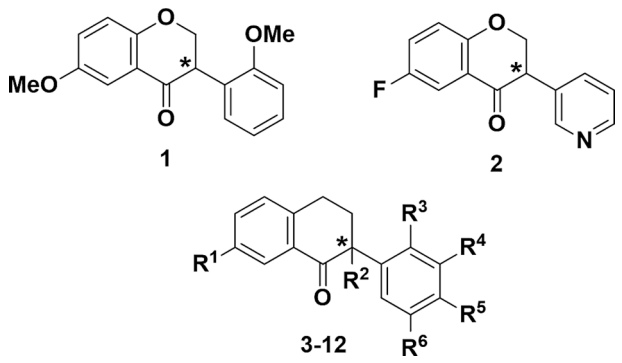

Fig. 1. Bioactive synthetic isoflavanones (**1** and **2**) and the 1-carba-analogues (**3**–**12**).

once pterocarpens and 5-carba-pterocarpens showed similar affinity for α and β estrogen receptors, being as potent as estradiol, the natural ligand [11]. In our group a synthetic aza-pterocarpan was active but less potent as antiproliferative on breast cancers and on leukemia cell lines when compared to its 1-carba-analogue [12]. Another interesting example is the substitution of the oxygen atom in prostacyclin (PGI2) by a methylene group. The carba-analogue showed the chemical stability greater than PGI2 and the same pharmacological activity profile. [13].

To design the new α-aryl-α-tetralones **3**–**12** (Fig. 2) we considered the therapeutic benefits that often result by the replacement of a hydrogen atom for a fluorine atom [14]. It is estimated that 20–25% of the drugs on the market have at least one fluorine atom in their structures [15]. The presence of this atom in a molecule can change bioabsorption, binding affinity, chemical reactivity, metabolic stability and, in some cases, can prevent the epimerization process [16–17]. In A-ring we maintained the same pattern of substitution used by Ma and coworkers.

At the B-ring we introduced different patterns of oxygenation, trying to improve the affinity of this ring for the Fe^{2+} present at the catalytic site of aromatase. The nitrile was selected considering the presence of this group in the structure of drugs employed for breast cancer therapy as aromatase inhibitors, such as letrozole and anastrozole. Finally, the presence of one fluorine atom at α-position in α-tetralone was proposed due to reasons already discussed.

Our target compounds are shown in Fig. 2. We report their synthesis, a preliminary evaluation of their potential antineoplastic activity on

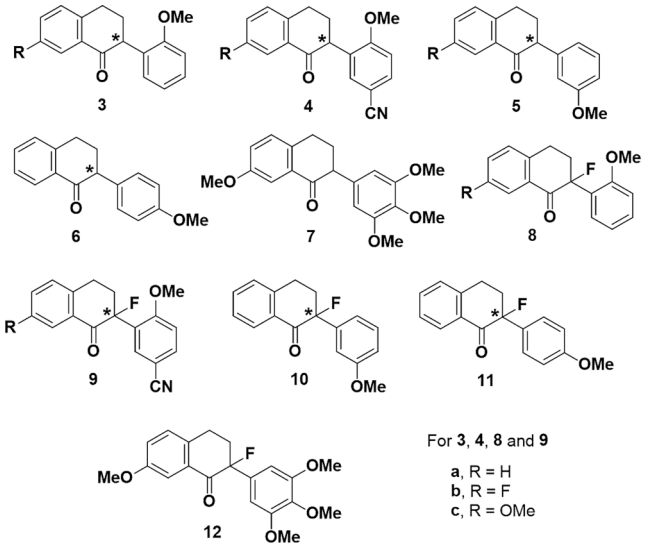

Fig. 2. New synthetic carba-analogues of isoflavanones with potential antiproliferative activity.

multidrug-resistant cell lines (MDR), the study of the efflux activity mediated by ABCB1 or ABCC1 proteins of the compounds with the lowest relative resistance indexes (RR) and the prediction of *in silico* ADMETox properties.

2. Results and discussion

Scheme 1 shows the α-aryl-α-tetralones **3**–**7** synthesized through a palladium catalyzed α-arylation reaction described by Fernandes *et al.* [18], using commercial α-tetralones and *o*-MeO-bromoarenes in the presence of $Pd_2(dba)_3$ as catalyst, tBu_3PHBF_4 as ligand and KOH with heating by microwave. Compounds **3a-c** were prepared in excellent yields under these conditions, but poor yields were observed for compounds **4**–**7**. In the case of compounds **4a-c**, we needed to increase the catalytic system to 5 mol% of $Pd_2(dba)_3$ and 20 mol% of tBu_3PHBF_4, and the temperature was raised to 130 °C. The other compounds, **5**–**7**, better yields were obtained when $Pd_2(dba)_3$ was changed for $Pd(dba)_2$ in the presence of NaOH.

The synthesis of the α-fluoro-α-aryl-α-tetralones (**8**–**12**) was initiated with the preparation of the corresponding α-fluoro-α-tetralones derivatives **15a-c** by α-fluorination of **13a-c** with Selectfluor in PEG-400. These compounds were prepared in good yield and were used in the α-arylation with **14a-e** (Scheme 2).

The structures were determined by ^1H and ^{13}C nuclear magnetic resonance (NMR) and mass spectroscopy, whereas a high-resolution mass spectrum was performed for the new compounds. In general, the ^1H NMR spectrum showed the α-carbonyl proton in 3.90–4.6 ppm as dd signals in α-aryl-α-tetralones (**3**–**7**) and none signal in this region for α-fluoro-α-aryl-α-tetralones (**8**–**12**). The aromatic protons signals appeared at 6.8–8.0 ppm and the aliphatic protons at 2.0–3.85 ppm as mutiplet signals. The ^{13}C spectrum showed duplicated signals in some carbon signals and the C-F had a coupling constant of approximately 200 Hz.

2.1. Biological evaluation

The synthesized compounds were evaluated for their antiproliferative effect on four human neoplastic cell lines with diverse phenotypes of drug resistance, and the results compared to the controls daunorubicin (**DNR**), a pro-oxidant, DNA-intercalating anthracycline and vincristine (**VCR**), a tubulin-binding antimitotic alkaloid. The cell lines employed in this study are specified as follows: MCF-7, an invasive, endocrine therapy-sensitive breast ductal carcinoma, estrogen and progesterone receptors positive and Her2/neu overexpression negative; K562, a chronic myeloid leukemia from erythroid origin with constitutive BCR/ABL tyrosine kinase activity, resistant to oxidative stress

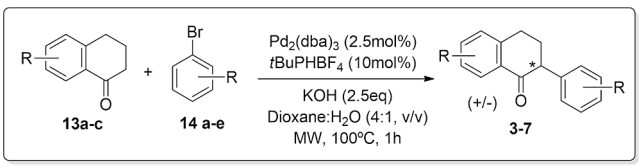

3a[1] 89% yield	**4a**[2] 45% yield	**5a**[3] 60% yield	**6**[3] 45% yield	**7**[3] 43% yield
3b[1] 92% yield	**4b**[2] 43% yield	**5c**[3] 54% yield		
3c[1] 90% yield	**4c**[2] 61% yield			

Scheme 1. Synthesis of α-aryl-α-tetralones **3**–**7**. [1]Reactions were carried out with ketone (0.2 mmol), bromo-aryl (0.24 mmol), $Pd_2(dba)_3$ (0.005 mmol), tBu_3PHBF_4 (0.02 mmol), and KOH (0.5 mmol) in dioxane:water (2.0 mL) for 1 h at 100 °C in MW. [2]Optimized conditions: 5 mol% $Pd_2(dba)_3$ (0.01 mmol), 20 mol% tBu_3PHBF_4 (0.04 mmol) and NaOH (0.5 mmol) for 1 h at 130 °C in MW. [3]Optimized conditions: 5 mol% $Pd(dba)_2$ (0.01 mmol), 10 mol% tBu_3PHBF_4 (0.02 mmol) and NaOH (0.5 mmol) for 1 h at 100 °C in MW.

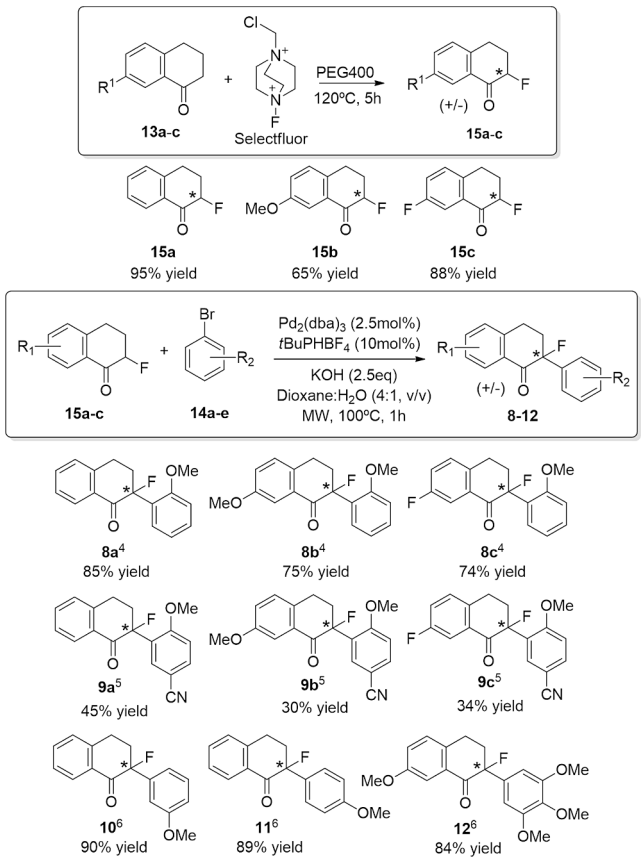

Scheme 2. Synthesis of α-fluoro-tetralones (**15a-c**) and α-fluoro-α-aryl-α-tetralones (**8**–**12**). [4]Reactions were carried out with fluoro-ketone (0.2 mmol), bromo-aryl (0.24 mmol) in dioxane:water (2.0 mL) for 1 h at 100 °C in MW. [5]Optimized mmol), $Pd_2(dba)_3$ (0.005 mmol), tBu_3PHBF_4 (0.02 mmol), and KOH (0.5 condition: 5 mol% $Pd_2(dba)_3$ (0.01 mmol), 20 mol% tBu_3PHBF_4 (0.04 mmol) and NaOH (0.5 mmol) for 1 h at 130 °C in MW. [6]Optimized condition: 5 mol% $Pd(dba)_2$ (0.01 mmol), 10 mol% tBu_3PHBF_4 (0.02 mmol) and NaOH (0.5 mmol) for 1 h at 100 °C in MW.

[19,20]; Lucena-1 and FEPS, multidrug resistant (MDR) K562 derivatives. Lucena-1 was selected after continuous exposure of K562 to VCR, resulting in ABCB1 (P-glycoprotein) overexpression and resistance to UV radiation and hydrogen peroxide [20]. FEPS was selected after continuous exposure of K562 to DNR, selecting cells resistant to a variety of natural and synthetic compounds owing to its high efflux activity mediated by the ABC transporters ABCB1 and ABCC1 (MRP1) [21]. The compounds were assessed in triplicate measurements and the mean IC_{50} values are presented in Table 1. MCF-10A, a spontaneously immortalized, non-tumorigenic and estrogen receptor negative human mammary epithelial cell [22] was employed for calculation of selectivity indices (SI) as well.

Concerning breast cancer, results showed that **8a** and **3b** inhibited the mitochondrial reducing activity of MCF-7 cells with the lowest IC_{50}, respectively 60.30 ± 7.41 μM and 66.87 ± 7.45 μM. Of note, both compounds present one fluorine atom in their structures, indicating that it could contribute to toxicity for breast cancer. In addition, **8a** presented the highest selectivity index (3.91), which demonstrates that this compound is more active in the tumor cell line MCF-7. Concerning chronic myeloid leukemias, notably **8a** and **8b** were the most promising compounds, with IC_{50} lower than 30 μM in the MDR FEPS cell. In agreement with previous results, both structures present α-fluorine atoms.

Leukemic cells showed lower IC_{50} for most compounds than breast cancer, suggesting differences in either drug distribution or in mechanisms of action on cells from epithelial or blood origins. The new α-aryl-α-tetralones and α-Fluoro-α-aryl-α-tetralones were proposed to interact

Table 1
Antineoplastic effect (IC_{50}) of synthesized compounds on models of human breast cancer and chronic myeloid leukemia.

Compound	MCF-7	MCF-10A	SI MCF-10A/ MCF-7	K562	Lucena-1	FEPS
3b	66.87 ± 7.45	152.67 ± 11.50	2.43	72.30 ± 8.03	63.17 ± 1.87	36.37 ± 2.05
3c	88.37 ± 6.00	172.22 ± 10.40	1.95	79.72 ± 2.57	58.02 ± 3.60	34.62 ± 1.73
8a	60.30 ± 7.41	235.67 ± 21.15	3.91	63.42 ± 4.68	46.84 ± 2.62	27.06 ± 1.28
8b	84.23 ± 4.70	>320	3.67	49.64 ± 3.06	39.00 ± 4.35	29.50 ± 1.51
DNR*	35.65 ± 5.56	61.57 ± 4.78	1.73	109.68 ± 3.58	2066.29 ± 138.82	>4000
VCR*	NA	NA	–	23.72 ± 0.39	405.61 ± 89.75	>960

Results are reported as IC_{50} values ± SD in μM. Data represent means obtained from three independent experiments, with each concentration evaluated in triplicates. Assays and calculations were performed as described in the Experimental Section. NA = Not analyzed. *For DNR and VCR, mean IC_{50} ± SD is expressed in nM rather than in μM.

with aromatase, the last and rate-limiting step in estrogen biosynthesis [9]. This is reasonable since we observed higher IC_{50} on MCF-7 than on MCF-10A, which does not rely on estrogens for proliferation. Myeloid leukemias express aromatase as well, and though estrogen metabolism was linked to hematopoiesis by regulating myeloid cell differentiation in two leukemia cell types [23–24], its role is not yet fully understood. However, considering the roles of estrogens as master regulators of cell bioenergetics [25], limiting its levels would disrupt mitochondrial function and lead cells to death due to ATP loss.

In addition, results indicated lower IC_{50} values for the drug-resistant leukemia FEPS, which reflected on the relative resistance indexes (RR). Increased sensitivity of MDR cells compared to parental ones is a form of synthetic lethality known as collateral sensitivity [26]. As such, RR were calculated for Lucena-1 and FEPS (Fig. 3) and when one compound showed RR ≤ 0.5 it was considered a collateral sensitizing agent [27]. When RR ≥ 2.0 cells were considered cross-resistant to a drug, which was the case for both Lucena-1 and FEPS when treated with the standard chemotherapeutics **VCR** or **DNR**.

Results on Fig. 3 indicate that despite α-aryl-α-tetralones and

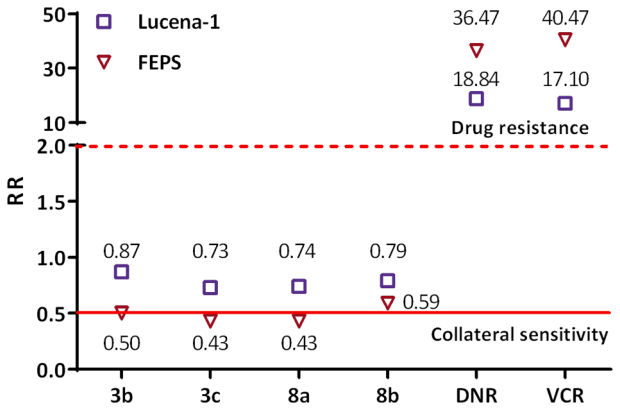

Fig. 3. Relative resistance (RR) indexes for the α-aryl-α-tetralones and α-fluoro-α-aryl-α-tetralones evaluated on chronic myeloid leukemias. Calculations were performed as described in the Experimental Section. RR = (IC_{50} resistant cell line, Lucena-1 or FEPS)/(IC_{50} parental cell line, K562). Purple squares and red inverted triangles respectively indicate Lucena-1 or FEPS, and the numbers indicate the calculated RR for each compound. (For interpretation of the references to colour in this figure legend, the reader is referred to the web version of this article.)

α-fluoro-α-aryl-α-tetralones presented lower IC_{50} on Lucena-1 when compared to K562, none induced collateral sensitivity. In contrast, **3b** as well as **3c** and **8a** produced this effect on FEPS cells. Studies with inhibitors of kinesin spindle proteins (KSP) have already linked the presence of halogens to higher cytotoxicity to drug-resistant cancer cells, in which the increase in bioavailability was important for this effect [28–29]. Moreover, inhibition of aromatase by anastrozole and letrozole was shown to induce increases in glutathione levels in breast cancer cells, likely to counter the oxidative stress after the depletion of estrogens [30]. On leukemias, and mostly on FEPS cells that overexpress ABCC1, this would possibly explain the increased sensitivity, since both impairment of energy production and increased efflux of glutathione (a prime ABCC1 substrate) are two possible inducers of collateral sensitivity [26,31]. Depletion of glutathione and ATP would render cells unable to deal with oxidative stress, leading them to apoptotic cell death [32,33].

So far, the synthesized α-aryl-α-tetralones and α-fluoro-α-aryl-α-tetralones exerted cytotoxicity regardless of the expression of the ABC proteins ABCB1 and ABCC1 on FEPS. To further investigate this possibility, we assessed if **3c** and **8a**, molecules with the lowest RR, would modulate the efflux activity by ABCB1 or ABCC1 on those cells. ABCB1 activity was measured by the efflux of rhodamine 123 (Rho 123) whereas ABCC1 was probed by the efflux of carboxyfluorescein (CF), the hydrolyzed form of 5(6)-carboxyfluorescein diacetate (CFDA). The MDR phenotype of both cells can be reversed by impairment of ABCB1 activity by the inhibitors verapamil (**VP**), trifluoperazine and cyclosporin A [20,21,32], or the ABCC1 inhibitors MK-571, indomethacin and probenecid [21,32]; as such, we employed VP and MK-571 as positive controls (Fig. 4).

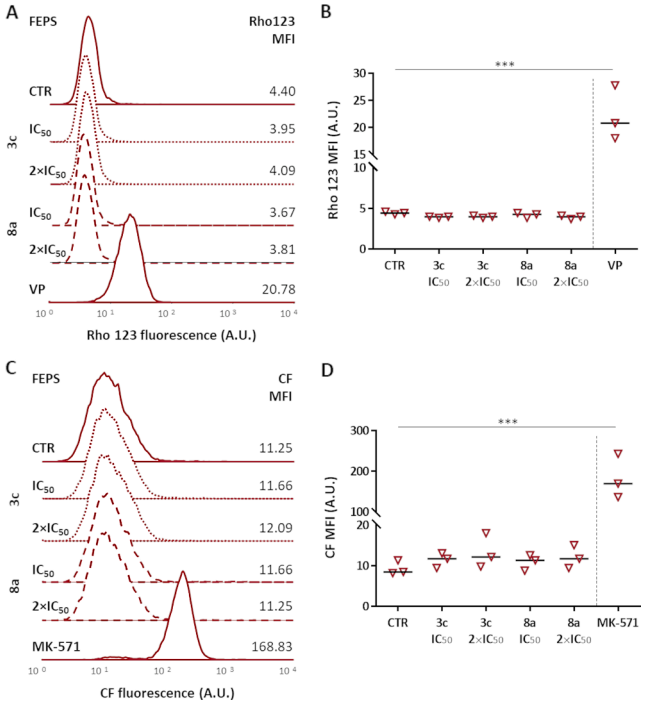

Fig. 4. Competition efflux assays of **3c** and **8a** for ABCB1 or ABCC1-mediated transport in FEPS cells. ABCB1 or ABCC1-mediated transport was evaluated by rhodamine 123 (Rho 123) or carboxyfluorescein (CF) efflux assays, as described in the Experimental Section. 10 μM verapamil (VP), 25 μM MK-571, standard inhibitors for ABCB1 and ABCC1, or concentrations equal to (IC_{50}) or two times the IC_{50} (2 × IC_{50}) of **3c** (35 and 70 μM) and **8a** (30 and 60 μM) were employed as competitive inhibitors. Representative histograms for intracellular (**A**) Rho 123 or (**C**) CF after efflux, with the median fluorescence intensities (MFI) listed on the right. Continuous lines indicate cells treated with diluent (CTR, free efflux) or with standard inhibitors (VP or MK-571, inhibited efflux). Dotted or dashed lines indicate cells, respectively, treated with **3c** or **8a** in the indicated concentrations. Scatter plots for the MFI obtained for (**B**) Rho 123 or (**D**) CF after the free, **3c–** or **8a-**competitive or after inhibited efflux. A.U., arbitrary units. Inverted triangles indicate FEPS cells, with lines indicating the median of each population. n = 3, with ***$p < 0.001$.

Results on Fig. 4 show that neither compound increased intracellular contents of Rho 123 or CF after incubations with concentrations equal to or double their IC_{50}. These profiles indicate that **3c** and **8a** are not substrates for ABCB1 or ABCC1, which is on par with our earlier observations. This would represent an interesting scenario for patients with endocrine therapy resistant cancers, since it has been described that ABCB1 actively extrudes anastrozole [34] and that little information is available concerning ABCC1. A variety of compounds exert collateral sensitization through increases in production of endogenous substrates of ABC transporters or directly by competitive inhibition [31–33]. Regardless of the latter not being observed here, monitoring of alterations associated with the onset of MDR but not directly ABC activity may provide clues to better understand our results.

2.2. *In silico analysis*

The compounds were evaluated according to the Lipinski "Rule of Five'' [35] and polar surface area (PSA) which is also a parameter for oral bioavailability. It was related that orally administered drugs with high PSA (>120 $Å^2$) were badly absorbed by passive transcellular route while drugs with low PSA (<60 $Å^2$) were well absorbed [36]. The values of molecular weight (270.10 to 288.09 Da), cLogP (3.63 to 4.04), HBD (0), HBA (2 to 3) and PSA (26.30 to 35.53 $Å^2$) showed in Table 2 were favorable for the evaluated compounds and may be well absorbed by oral route. The results were compared to the chemotherapeutic drugs daunorubicin (**DNR**) and vincristine (**VCR**). We also calculated the druglikeness, that evaluates whether the molecule contains predominantly fragments commonly present in commercial drugs in comparison to non-drug-like collection of Fluka compounds. All compounds showed negative druglikeness (-7.22 to −0.87), which demonstrated the presence of uncommon fragments compared to traded drugs as well as to commercially available chemicals (Fluka).

It is important to freezing the changes of fluorine substituent in the molecules and the similarities of the molecules that presented the antiproliferative results. These compounds have similarities in the physicochemical properties which have the same values of PSA (26.30) and HBA (2) that may indicate the same mechanism of action and the need for low PSA and HBA values.

The analysis of theoretical potential toxicity risks of the compounds showed similar characteristics, with no risks of mutagenic, tumorigenic and irritating effects and high risk of reproductive effect for all compounds, comparable to the standard antineoplastic drugs **VCR** and **DNR** (data not shown). These predictions processes are based on the analysis of fragments of the structure designed and compared to a list of fragments created by the program, based on the assumption that commercial drugs are largely free of toxic effects. Any fragment was considered a risk

Table 2
Calculated physicochemical properties.

Comp.	AMW[a]	PSA[b]	HBA[c]	HBD[d]	cLogP[e]	Druglikeness
3b	270.10	26.30	2	0	4.04	−2.21
3c	282.12	35.53	3	0	3.87	−0.87
8a	270.10	26.30	2	0	3.63	−7.22
8b	288.09	26.30	2	0	3.73	−7.22
DNR	527.18	185.84	11	5	1.09	6.16
VCR	824.40	171.17	14	3	2.98	4.03

[a] AMW, absolute molecular weight.
[b] PSA, polar surface area.
[c] HBA, hydrogen bond acceptor.
[d] HBD, hydrogen bond donor.
[e] cLogP, calculated logarithm of partition coefficient between *n*-octanol and water.

factor if it occurred often as substructures of harmful compounds but never or rarely in commercial drugs.

3. Conclusion

A series of α-aryl-α-tetralones and α-fluoro-α-aryl-α-tetralones (1-carba-isoflavanone analogues) were synthesized with moderate to good yields, up to 92%. Some compounds were evaluated for cytotoxicity toward human breast cancer and chronic myeloid leukemias with diverse profiles of drug resistance. Concerning breast cancer, **8a** and **3b** showed the best anti-proliferative results with the first, with a fluorine atom in a chiral center, presenting the highest selectivity. **8a** and **3c**, both with fluorine substitutions, showed the most promising results for chronic myeloid leukemias, notably for the MDR cell FEPS when compared to the drug-sensitive K562. This feature, known as collateral sensitivity, has been observed in several other classes of compounds and relates to changes in energy metabolism, membrane fluidity and mechanisms of drug efflux. In this context, the α-aryl-α-tetralone **3b** and the α-fluoro-α-aryl-α-tetralone **8a** exerted cytotoxicity by evading the two most common ABC transporters. The *in silico* analysis of ADMETox properties revealed that the compounds meet the criteria to be well absorbed following oral administration, with reduced probability of toxic effects. Therefore, these compounds exhibit interesting properties for the development of pharmaceutical agents aimed to chemotherapy-refractory cancers.

4. Experimental

4.1. General

Reagents and solvents were obtained commercially and used without further purification. The microwave-assisted reactions were conducted on a single-mode Discover System from CEM Discover and Explorer-Coolmate accessory. NMR spectra were recorded in deuterated chloroform, unless otherwise stated, on a spectrometer operating at 400 MHz ^{1}H NMR, 101 MHz ^{13}C NMR and 470 MHz ^{19}F (spectra were recorded using Varian INOVA 400 MHz and Varian INOVA 500 MHz) with tetramethylsilane (TMS) and chloroform as internal standards. Chemical shifts are reported as δ values (ppm). The following abbreviations are used for the multiplicities: s: singlet, d: doublet, dd: doublet of doublet, t: triplet, q: quadruplet, m: multiplet. High resolution mass spectra (GC-EI) were recorded using a QTOF Agilent 7200 instrument for the exact mass and Agilent 7890B for the GC. The progress of reactions was monitored by thin layer chromatography (TLC) and column chromatography were carried out on silica gel, the flash column chromatography silica gel 60 (40–60 mm) was employed. Analytical TLC was done using ALUGRAM® Xtra SIL G/ UV_{254} silica gel plates, and the spots were determined under UV light (λ = 254 nm).

4.2. Synthesis of α-aryl-α-tetralones

4.2.1. General procedure for the synthesis of α-aryl-α-tetralones

In a microwave tube were added a suspension of $Pd(dba)_2$ (0.0057 g, 0.01 mmol), tBu$_3$PHBF$_4$ (0.0058 g, 0.02 mmol), NaOH (0.016 g, 0.4 mmol), aryl bromide (0.24 mmol) and α-tetralone (0.2 mmol) in a mixture of degassed dioxane/water (4:1, v/v, 2 mL) and heated under argon atmosphere and microwave irradiation (100 W of initial power, 100–130 °C, 60 min, infrared probe). Then, the mixture was allowed to cool to rt, diluted in AcOEt, washed with saturated NH_4Cl solution, dried over anhydrous $NaSO_4$, filtered and concentrated under reduced pressure. The crude material was purified by silica gel column with hexane: AcOEt (95:5) as solvent.

Compounds **3a** [18], **3b** [17], **3c** [18], **5a** [37], **6a** [37] are known, new compounds follow:

*4.2.1.1. 4-methoxy-3-(1-oxo-1,2,3,4-tetrahydronaphthalen-2-yl)benzonitrile (**4a**): Yellow solid (25 mg, 45%).* Mp: 159–161 °C.^{1}H NMR (400 MHz, $CDCl_3$) δ 8.07 (d, J = 7.7 Hz, 1H), 7.59 (dd, J = 8.6, 2.0 Hz, 1H), 7.52 (t, J = 7.4 Hz, 1H), 7.41 (d, J = 1.9 Hz, 1H), 7.35 (t, J = 7.5 Hz, 1H), 7.30 (d, J = 7.7 Hz, 1H), 6.96 (d, J = 8.6 Hz, 1H), 4.07 (dd, J = 12.9, 4.5 Hz, 1H), 3.82 (s, 3H), 3.18 (ddd, J = 16.5, 12.3, 4.3 Hz, 1H), 3.05 (dt, J = 16.6, 3.7 Hz, 1H), 2.49 (ddd, J = 25.3, 12.8, 4.3 Hz, 1H), 2.30 – 2.23 (m, 1H); ^{13}C NMR (101 MHz, $CDCl_3$) δ 196.75, 160.53, 143.82, 133.52, 133.14, 133.10, 132.54, 130.48, 128.78, 127.66, 126.81, 119.28, 111.26, 103.97, 55.80, 49.67, 29.69, 29.48. HRMS (ESI): *m/z* calcd. for $C_{18}H_{15}NO_2$: 277.1103; found: 277.1094.

*4.2.1.2. 3-(7-fluoro-1-oxo-1,2,3,4-tetrahydronaphthalen-2-yl)-4-methoxybenzonitrile (**4b**).* yellow solid (36 mg, 61%). Mp: 162–166 °C.^{1}H NMR (400 MHz, $CDCl_3$) δ 7.69 (dd, J = 9.1, 2.4 Hz, 1H), 7.57 (dd, J = 8.5, 1.5 Hz, 1H), 7.38 (d, J = 1.4 Hz, 1H), 7.29 – 7.24 (m, 1H), 7.20 (td, J = 8.2, 2.5 Hz, 1H), 6.94 (d, J = 8.6 Hz, 1H), 4.00 (dd, J = 13.0, 4.4 Hz, 1H), 3.79 (s, 3H), 3.16 – 3.06 (m, 1H), 3.01 (dt, J = 16.4, 3.4 Hz, 1H), 2.51 – 2.40 (m, 1H), 2.28 – 2.20 (m, 1H); ^{13}C NMR (101 MHz, $CDCl_3$) δ 195.67 (d, J = 1.8 Hz), 162.79, 160.40 (d, J = 11.2 Hz), 139.52 (d, J = 3.0 Hz), 134.10 (d, J = 6.1 Hz), δ 133.20 (d, J = 2.1 Hz), 133.18 – 133.07 (m), 130.62 (d, J = 7.1 Hz), 130.16, 120.82 (d, J = 22.2 Hz), 119.17, 113.48 (dd, J = 21.8, 4.6 Hz), 111.34, 104.05, 55.81, 49.53, 29.42, 28.79. HRMS (ESI): *m/z* calcd. for $C_{18}H_{14}FNO_2$: 295.1009; found: 295.1003.

*4.2.1.3. 4-methoxy-3-(7-methoxy-1-oxo-1,2,3,4-tetrahydronaphthalen-2-yl)benzonitrile (**4c**).* yellow solid (26.4 mg, 43%). Mp: 155–158 °C.^{1}H NMR (400 MHz, $CDCl_3$) δ 7.59 (dd, J = 8.5, 1.8 Hz, 1H), 7.55 (d, J = 2.6 Hz, 1H), 7.40 (d, J = 1.6 Hz, 1H), 7.22 (d, J = 8.4 Hz, 1H), 7.10 (dd, J = 8.4, 2.7 Hz, 1H), 6.96 (d, J = 8.6 Hz, 1H), 4.04 (dd, J = 12.8, 4.4 Hz, 1H), 3.85 (s, 3H), 3.83 (s, 3H), 3.10 (ddd, J = 16.2, 12.2, 4.2 Hz, 1H), 2.98 (dt, J = 16.4, 3.6 Hz, 1H), 2.46 (qd, J = 12.6, 4.2 Hz, 1H), 2.28 – 2.21 (m, 1H); ^{13}C NMR (101 MHz, $CDCl_3$) δ 196.69, 160.55, 158.40, 136.44, 133.32, 133.05, 130.56, 129.99, 121.79, 119.25, 111.23, 109.64, 109.62, 109.59, 103.99, 55.80, 55.49, 49.49, 29.68, 28.62. HRMS (ESI): *m/z* calcd. for $C_{19}H_{17}NO_3$: 307.1208; found: 307.1198.

*4.2.1.4. 7-methoxy-2-(3-methoxyphenyl)-3,4-dihydronaphthalen-1(2H)-one (**5c**).* brown oil (30.4 mg, 54%).^{1}H NMR (300 MHz, $CDCl_3$) δ 7.57 (d, J = 2.8 Hz, 1H), 7.25 (t, J = 7.9 Hz, 1H), 7.19 (d, J = 8.4 Hz, 1H), 7.08 (dd, J = 8.4, 2.8 Hz, 1H), 6.81 (ddd, J = 8.3, 2.5, 0.9 Hz, 1H), 6.79 – 6.72 (m, 2H), 3.84 (s, 3H), 3.78 (s, 3H), 3.74 (d, J = 7.8 Hz, 1H), 3.09 – 2.92 (m, 2H), 2.39 (ddd, J = 7.9, 6.3, 3.6 Hz, 2H). ^{13}C NMR (75 MHz, $CDCl_3$) δ 198.01, 159.66, 158.41, 141.34, 136.69, 133.59, 130.00, 129.47, 121.81, 120.79, 114.45, 112.15, 109.66, 55.50, 55.16, 54.20, 31.40, 27.84. HRMS (ESI): *m/z* calcd. for $C_{18}H_{18}O_3$: 282.1256; found: 282.1259.

*4.2.1.5. 7-methoxy-2-(3,4,5-trimethoxyphenyl)-3,4-dihydronaphthalen-1(2H)-one (**7**).* green solid (29.5 mg, 43%). Mp: 176–178 °C.^{1}H NMR (300 MHz, $CDCl_3$) δ 7.58 (d, J = 2.8 Hz, 1H), 7.22 (d, J = 8.4 Hz, 1H), 7.14–7.07 (m, 1H), 6.41 (s, 2H), 3.85 (s, 3H), 3.85 (s, 3H), 3.83 (s, 6H), 3.14–2.94 (m, 2H), 2.46–2.34 (m, 2H). ^{13}C NMR (75 MHz, $CDCl_3$) δ 198.09, 158.39, 153.17, 136.77, 136.65, 135.61, 133.48, 130.03, 121.83, 109.67, 105.44, 60.80, 56.01, 55.50, 54.77, 31.72, 28.24. HRMS (ESI): *m/z* calcd. for $C_{20}H_{22}O_5$: 342.1467; found: 342.1484.

4.2.2. General procedure for the synthesis of α-fluoro-α- aryl-α-tetralones

In a microwave tube were added a suspension of Selectfluor (0.5314 g, 1.5 mmol) and α-tetralone (1.0 mmol) in PEG400 (2 mL) and thermal heated at 120 °C. Then, the mixture was allowed to cool to rt, diluted in AcOEt, washed with brine, dried over anhydrous $NaSO_4$, filtered and concentrated under reduced pressure. The crude material was purified by silica gel column with hexane:AcOEt (95:5) as solvent. Compounds **15a** [38], **15b** [39], **15c** [40] are known.

Before the first step, in a microwave tube were added a suspension Pd $(dba)_2$ (0.0057 g, 0.01 mmol), tBu_3PHBF_4 (0.0058 g, 0.02 mmol), NaOH (0.016 g, 0.4 mmol), aryl bromide (0.24 mmol) and compounds **9a-b** (0.2 mmol) in a mixture of degassed dioxane/water (4:1, v/v, 4 mL) and heated under argon atmosphere and microwave irradiation (100 W of initial power, 100–130 °C, 60 min, infrared probe). Then, the mixture was allowed to cool to rt, diluted in AcOEt, washed with saturated NH_4Cl solution, dried over anhydrous $NaSO_4$, filtered and concentrated under reduced pressure. The crude material was purified by silica gel column with hexane:AcOEt (95:5) as solvent.

Compounds **8a** [17], **8b** [17], **8c** [17], **10** [41], **11** [17] are known, new compounds follow:

*4.2.2.1. 3-(2-fluoro-1-oxo-1,2,3,4-tetrahydronaphthalen-2-yl)-4-methoxybenzonitrile (**9a**).* light brown solid (28 mg, 47%). Mp: 179–182 °C. ^{1}H NMR (400 MHz, $CDCl_3$) δ 8.07 (d, J = 7.8 Hz, 1H), 7.87 (d, J = 1.7 Hz, 1H), 7.64 (dd, J = 8.6, 1.9 Hz, 1H), 7.54 (t, J = 7.5 Hz, 1H), 7.37 (t, J = 7.6 Hz, 1H), 7.30 (d, J = 7.6 Hz, 1H), 6.92 (d, J = 8.5 Hz, 1H), 3.65 (s, 3H), 3.40 – 3.30 (m, 1H), 2.95 – 2.76 (m, 2H), 2.44 – 2.34 (m, 1H); ^{13}C NMR (101 MHz, $CDCl_3$) δ 189.56 (d, J = 18.7 Hz), 158.05 (d, J = 6.2 Hz), 143.33, 134.23, 134.02, 130.93, 130.49 (d, J = 22.7 Hz), 130.18 (d, J = 15.8 Hz), 128.65, 128.41, 127.16, 118.96, 111.80 (d, J = 1.8 Hz), 104.63 (d, J = 2.5 Hz), 94.15 (d, J = 179.0 Hz), 55.84, 33.99 (d, J = 23.5 Hz), 24.70 (d, J = 3.8 Hz); ^{19}F NMR (470 MHz, $CDCl_3$)δ −165.41 (dd, J = 42.5, 13.4 Hz). .HRMS (ESI): m/z calcd. for $C_{18}H_{14}FNO_2$: 295.1009; found: 295.1003.

*4.2.2.2. 3-(2,7-difluoro-1-oxo-1,2,3,4-tetrahydronaphthalen-2-yl)-4-methoxybenzonitrile (**9b**).* light yellow solid (21.3 mg, 34%).Mp: 154–158 °C. ^{1}H NMR (400 MHz, cdcl$_3$) δ 7.89 (d, J = 1.7 Hz, 1H), 7.75 (dd, J = 8.9, 2.4 Hz, 1H), 7.67 (dd, J = 8.5, 1.9 Hz, 1H), 7.30 (dt, J = 8.1, 5.5 Hz, 2H), 6.95 (d, J = 8.5 Hz, 1H), 3.68 (s, 3H), 3.31 (dd, J = 20.1, 6.1 Hz, 1H), 2.91 – 2.78 (m, 2H), 2.41 (ddd, J = 8.7, 8.0, 3.0 Hz, 1H).^{13}C NMR (101 MHz, cdcl$_3$) δ 188.63 (dd, J = 18.6, 1.7 Hz), 161.75 (d, J = 247.0 Hz), 157.90 (d, J = 6.1 Hz), 139.09 (d, J = 3.1 Hz), 134.33, 132.42 (d, J = 6.5 Hz), 130.56 (d, J = 7.1 Hz), 130.34 – 130.03 (m), 121.45 (d, J = 22.2 Hz), 118.85, 114.17 (d, J = 22.1 Hz), 111.82 (d, J = 1.7 Hz), 104.80 (d, J = 1.4 Hz), 93.62 (dd, J = 179.2, 0.9 Hz), 55.87, 34.02 (d, J = 23.6 Hz), 29.68 (s), 24.05 (d, J = 3.9 Hz).^{19}F NMR (470 MHz, $CDCl_3$) δ −113.93 (dd, J = 14.1, 7.8 Hz), −165.67 (dd, J = 43.0, 13.4 Hz).HRMS (ESI): m/z calcd. for $C_{18}H_{13}F_2NO_2$: 313.0914; found: 313.0911.

*4.2.2.3. 3-(2-fluoro-7-methoxy-1-oxo-1,2,3,4-tetrahydronaphthalen-2-yl)-4-methoxybenzonitril (**9c**).* light brown solid (19.5 mg, 30%). Mp: 150–155 °C.^{1}H NMR (400 MHz, cdcl$_3$) δ 7.89 (d, J = 1.8 Hz, 1H), 7.67 (dd, J = 8.5, 2.0 Hz, 1H), 7.56 (d, J = 2.7 Hz, 1H), 7.23 (d, J = 8.5 Hz, 1H), 7.14 (dd, J = 8.4, 2.7 Hz, 1H), 6.94 (d, J = 8.6 Hz, 1H), 3.86 (s, 3H), 3.69 (s, 3H), 3.30 (td, J = 11.0, 4.7 Hz, 1H), 2.90 – 2.75 (m, 2H), 2.43 – 2.35 (m, 1H).^{13}C NMR (101 MHz, cdcl$_3$) δ 189.39 (d, J = 18.6 Hz), 158.67 (s), 158.09 (d, J = 6.1 Hz), 136.01 (s), 134.19 (s), 131.64 (s), 130.55 (d, J = 22.7 Hz), 130.23 (d, J = 15.9 Hz), 129.90 (s), 122.33 (s), 118.92 (s), 111.77 (s), 110.31 (s), 104.69 (s), 94.02 (d, J = 179.1 Hz), 55.86 (s), 55.54 (s), 34.17 (d, J = 23.5 Hz), 29.67 (s), 23.94 (d, J = 3.7 Hz).^{19}F NMR (470 MHz, $CDCl_3$) δ −165.38 (dd, J = 42.6, 13.2 Hz). HRMS (ESI): m/z calcd. for $C_{19}H_{16}FNO_3$: 325.1114; found: 325.1111.

*4.2.2.4. 2-fluoro-7-methoxy-2-(3,4,5-trimethoxyphenyl)-3,4-dihydronaphthalen-1(2H)-one (**12**).* green solid (60.3 mg, 84%). Mp: 128–129 °C.^{1}H NMR (300 MHz, $CDCl_3$) δ 7.61 (d, J = 2.5 Hz, 1H), 7.17 (d, J = 8.5 Hz, 1H), 7.12 (dd, J = 8.5, 2.6 Hz, 1H), 6.56 (d, J = 0.9 Hz, 2H), 3.87 (s, 3H), 3.83 (s, 3H), 3.78 (s, 6H), 3.14 – 2.99 (m, 1H), 2.92 – 2.78 (m, 1H), 2.75 – 2.58 (m, 2H). ^{13}C NMR (75 MHz, $CDCl_3$) δ 193.52 (d, J = 18.5 Hz), 158.73, 153.22, 138.58 (d, J = 2.5 Hz), 135.74, 132.82, 132.22, 132.07 (d, J = 23.0 Hz), 131.91, 130.13, 122.89, 109.57, 103.46 (d, J = 6.2 Hz), 95.96 (d, J = 184.8 Hz), 60.81, 56.15, 55.61, 35.67 (d, J = 25.0 Hz), 25.66 (d, J = 9.3 Hz).^{19}F NMR (470 MHz, $CDCl_3$) δ −144.17 (t, J = 10.9 Hz).HRMS (ESI): m/z calcd. for $C_{20}H_{21}FO_5$: 360.1373; found: 360.1387.

4.3. Biological evaluation

4.3.1. Cell lines

Breast cancer cells MCF-7 were cultured in high glucose DMEM medium (Gibco, Grand Island, NY, USA) 10 g/L supplemented with 25 mM HEPES, 0.584 g/L glutamine, 100 mg/L streptomycin and 60 mg/L penicillin (all from Sigma-Aldrich). MCF-10A epithelial breast cells were cultured in complete MEGM Mammary Epithelial Cell Growth Medium (Lonza, Basel, Switzerland), containing the epidermal growth factor and insulin needed for stimulating cell proliferation. All media was supplemented with 10% fetal bovine serum (FBS) (Cultilab, São Paulo, Brazil) inactivated at 56 °C for 1 h prior to use. The chronic myeloid leukemia cell lines K562, Lucena-1 and FEPS were cultured in RPMI-1640 medium (Gibco BRL, Paisley, UK) supplemented with 25 mM HEPES adjusted to pH 7.4 with NaOH, 60 mg/L penicillin and 100 mg/L streptomycin (all obtained from Sigma-Aldrich). Briefly, K562 cells were exposed to increasing concentrations of the chemotherapeutic drugs vincristine sulfate and daunorubicin hydrochloride (DNR) (both from Sigma-Aldrich), as described before [20,21]. Lucena-1 (K562/VCR) and FEPS (K562/DNR) were cultured, respectively, in the presence of either 60 nM VCR or 500 nM DNR in order to maintain the MDR phenotypes. For subcultures, cells were harvested every 3 days by incubation with (for breast cells) or without (for leukemias) 2.5 mg/mL trypsin (Sigma-Aldrich) at 37 °C, followed by washing with cold FBS, and maintained at 37 °C in 5% CO_2.

4.3.2. Evaluation of mitochondrial reducing activity

Mitochondrial reducing activity was determined by the 3-(4,5-dimethylthiazol-2-yl)-2,5-diphenyltetrazolium (MTT; Sigma-Aldrich) colorimetric assay. MCF-7 and MCF-10A cells (2×10^4 mL^{-1}) were allowed to adhere to 96-well plates for 24 h. Adhered breast cells or leukemia cells (2×10^4 mL^{-1}) were incubated for 72 h at 37 °C, followed by treatment with compounds at a range of concentrations. MTT (5 mg/mL) was added to each well, and plates were kept at 37 °C in 5% CO_2 for 3 h. After centrifugation, 200 μL of DMSO was added to dissolve the dark-blue formazan crystals formed by MTT reduction. Absorbance was measured by enzyme-linked immunosorbent assay (ELISA) on a plate reader (Sunrise; Tecan Group Ltd., Männedorf, Switzerland) at 570 nm, with absorbance being directly proportional to formazan content and indicative of living cells. The half-maximal inhibitory concentrations (IC_{50}) were calculated by non-linear regression using the GraphPad Prism version 7.0 program (GraphPad Software, San Diego, CA, USA). The selectivity index (SI) for breast cancer cells was calculated using the formula **(SI) = (IC_{50} MCF-10A)/(IC_{50} MCF-7)**. When IC_{50} exceeded the maximal tested concentration, it was expressed as being higher than this concentration (e.g. > 320), and this value was used for calculating the SI (e.g. SI of **8b** towards MCF-7: IC_{50} MCF-10A / IC_{50} MCF-7 = 320/84.23 = 3.67). Alternatively, the relative resistance (RR) was calculated using the formula **(RR) = (IC_{50} MDR cell line, Lucena-1 or FEPS) / (IC_{50} parental cell line, K562)**. Similarly, values expressed as being higher than a concentration were used for calculating the RR (e.g. RR of VCR toward FEPS: IC_{50} FEPS / IC_{50} K562 = 960/23.72 = 40.47). If RR ≤ 0.5, the compound exerted collateral sensitivity, and cells were considered cross-resistant when RR ≥ 2.0 [27].

4.3.3. ABC-mediated efflux assays

The ABCB1 and ABCC1 transport assays were performed, respectively, with the use of the rhodamine 123 (Rho 123) and 5(6)-carboxyfluorescein diacetate (CFDA) dyes (both from Sigma-Aldrich) as previously described [32]. Rho 123 and CFDA passively distribute into the cell, and while the first is fluorescent and is actively extruded by ABCB1, the latter undergoes hydrolysis by nonspecific esterases in the

cytosol, originates the fluorescent substrate carboxyfluorescein (CF) that only then is transported out by ABCC subfamily members, notably ABCC1 [42]. Briefly, assays were performed in two 30-minute steps, sufficient for the accumulation and efflux of dyes. Both steps were carried on at 37 °C in 5% CO_2 in a light-protected environment. First, 2×10^5 FEPS cells were incubated in 96-well plates with 250 nM Rho 123 or 500 nM CFDA in presence of **3c** or **8a** in concentrations equal to or two times the IC_{50} toward FEPS, diluted in RPMI medium to allow accumulation of the dyes within cells (accumulation phase). Following, cells were centrifuged at 200 × g for 7 min and then resuspended in fresh RPMI medium to allow efflux of the dyes (efflux phase). Inhibition of ABCB1 efflux was performed in the presence of the calcium channel blocker verapamil (VP) [43], and the quinoline derivative MK-571 was employed to inhibit ABCC efflux [44] (inhibited efflux). As negative control, cells were exposed to medium only (free efflux). Then, cells were again centrifuged, resuspended in cold PBS and maintained on ice until acquisition by flow cytometry.

4.3.4. Flow cytometry

The median fluorescence intensities (MFI) from 15,000 viable cells, gated in accordance with forward and side scatter parameters representative of cell size and granularity, were acquired using the FL1-H filter on a BD FACSCalibur flow cytometer (BD Biosciences, San Jose, CA, USA) and represented on histograms. All post-analysis was performed on Summit version 4.3 software (Dako Colorado, Inc., Fort Collins, CO, USA).

4.3.5. Statistical analysis

Statistical analyses were performed using GraphPad Prism version 7.0 software. The paired one-way ANOVA, the Friedman test and the Dunn's post-test were employed for analysis of nonparametric data. Null hypotheses were rejected when p-values were lower than 0.05, and significances were represented by (*) for $p < 0.05$, (**) for $p < 0.01$ and (***) for $p < 0.001$.

4.4. In silico analysis

The theoretical physicochemical parameters related to absorption, distribution, metabolism, and excretion (ADME) were built and optimized using the software Spartan'10 (Wavefunction Inc. Irvine, CA, 2000). First of all, the conformational analysis was performed using molecular mechanics with Merck Molecular Force Field (MMFF94). Before, the geometry optimization was performed using Recife Model 1 (RM1) semi-empirical method, and finally the stereoelectronic properties of compounds were calculated with Hartree-Fock method using the basis set 6-311G*. The descriptors calculated include absolute molecular weight (AMW), polar surface area (PSA), number of hydrogen bond donors (HBD) and acceptors (HBA) groups. We also calculated octanol water partition coefficient (clogP) and druglikeness using Osiris Property Explorer program (http://www.organic-chemistry.org) which evaluates the chemical structure of the molecule and compares whether it contains fragments commonly present in commercial drugs and non-drug-like collection of Fluka compounds. The toxicity risks of the compounds were also evaluated using Osiris Property Explorer [45] and include mutagenic, tumorigenic, irritant and reproductive effects.

Declaration of Competing Interest

The authors declared that there is no conflict of interest.

Acknowledgments

Financial support from Brazilian agencies CAPES, CNPq, FAPERJ and UFRJ is acknowledged. L. G. S. thanks CAPES for the fellowship.

Appendix A. Supplementary data

Supplementary data to this article can be found online at https://doi.org/10.1016/j.bioorg.2021.104790.

References

[1] D. Hanahan, R.A. Weinberg, Hallmarks of cancer: the next generation, Cell 144 (5) (2011) 646–674.
[2] R.L. Siegel, K.D. Miller, A. Jemal, Cancer statistics, CA Cancer J. Clin. 68 (2018) (2018) 7–30.
[3] R. Baan, Y. Grosse, K. Straif, B. Secretan, F. El Ghissassi, V. Bouvard, L. Benbrahim-Tallaa, N. Guha, C. Freeman, L. Galichet, V. Cogliano, A review of human carcinogens – part F: chemical agents and related occupations, Lancet Oncol. 10 (12) (2009) 1143–1144.
[4] V. Bouvard, R. Baan, K. Straif,Y. Grosse, B. Secretan, F. El Ghissassi, L. Benbrahim-Tallaa, N. Guha, C. , L. Galichet, V. Cogliano, A review of human carcinogens – part B: biological agents,LancetOncol. 10(12) (2009) 321–322.
[5] João Pedro de Magalhães, How ageing processes influence cancer, Nature Rev. Cancer 13 (5) (2013) 357–365.
[6] Caitriona Holohan, Sandra Van Schaeybroeck, Daniel B. Longley, Patrick G. Johnston, Cancer drug resistance: an evolving paradigm, Nature Rev. Cancer 13 (10) (2013) 714–726.
[7] L.H. Yao, Y.M. Jiang,J. Shi, F.A. Tomás-Barberán, N. Datta, R. Singanusong, S.S. Chen, Flavonoids in Food and Their Health Benefits, Plant Foods Hum. Nutri.59 (2004)113–122.
[8] C. Kanadaswami, L.-T. Lee, P.-P.H. Lee, J.-J. Hwang, F.-C. Ke, Y.-T. Huang, M.-T. Lee, The Antitumor Activities of Flavonoids, Vivo 19 (2005) 895–910.
[9] K. Bonfield, E. Amato, T. Bankemper, H. Agard, J. Steller, J.M. Keeler, D. Roy, A. McCallum, S. Paula, L. Ma, Development of a new class of aromatase inhibitors: design, synthesis and inhibitoryactivity of 3-phenylchroman-4-one (isoflavanone) derivatives, Bioorg. Med. Chem. 20 (2012) 2603–2613.
[10] E. Amato, T. Bankemper, R. Kidney, T. Do, A. Onate, S. Thowfeik, E.J. Merino, S. Paula, L. Ma, Investigation of fluorinated and bifunctionalized 3-phenylchroman-4-one (isoflavanone) aromatase inhibitors, Bioorg. Med. Chem. 22 (2014) 126–134.
[11] C.P.Miller, M.D. Collini, R.L. Morris, R.R. Singhaus, US 20060004087, U.S. Pat. Appl. Publ. (2006).
[12] C.D. Buarque, E.J. Salustiano, K.C. Fraga, B.R.M. Alves, P.R.R. Costa, 11a-N-Tosyl-5-deoxi-pterocarpan (LQB-223), a promising prototype for targeting MDR leukemia cell lines, Euro. J. Med. Chem. 78 (2014) 190–197.
[13] Werner Skuballa, Helmut Vorbrüggen, A New Route to 6a-Carbacyclins–Synthesis of a Stable, Biologically Potent Prostacyclin Analogue, Angew. Chem. Int. Ed. Engl. 20 (12) (1981) 1046–1048.
[14] Jeremy Erb, Ethan Alden-Danforth, Nathan Kopf, Michael T. Scerba, Thomas Lectka, Combining Asymmetric Catalysis with Natural Product Functionalization through Enantioselective α-Fluorination, J. Org. Chem. 75 (3) (2010) 969–971.
[15] Sophie Purser, Peter R. Moore, Steve Swallow, Véronique Gouverneur, Fluorine in Medicinal Chemistry, Chem. Soc. Rev. 37 (2) (2008) 320–330.
[16] H.-J. Böhm, D. Banner, S. Bendels, M. Kansy, B. Kuhn, K. Müller, U. Obst-Sander, M. Stahl, Fluorine in medicinal chemistry, Chem. Bio. Chem. 5 (2004) 637–643.
[17] L.G. Souza, J.L.O. Domingos, T.A. Fernandes, M.N. Renno, J.M. Sansano, C. Najera, P.R.R. Costa, Enantioselective electrophilic fluorination of -aryl-tetralones using a preparation of N-fluoroammonium salts of cinchonine, J. Fluor. Chem. 217 (2019) 72–79.
[18] Talita de A. Fernandes, Jorge L.O. Domingos, Luiza I.A. da Rocha, Sabrina de Medeiros, Carmen Nájera, Paulo R.R. Costa, Synthesis of 5-Carbapterocarpens by α-Arylation of Tetralones Followed by One-Pot Demethylation/Cyclization with BBr 3, Eur. J. Org. Chem. 2014 (6) (2014) 1314–1320.
[19] Y.-P. Chau, S.-G. Shiah, M.-J. Don, M.-L. Kuo, Involvement of hydrogen peroxide in topoisomerase inhibitor b-lapachone-induced apoptosis and differentiation in human leukemia cells, Free Radical Biol. Med. 24 (4) (1998) 660–670.
[20] V.M. Rumjanek, G.S. Trindade, K. Wagner-Souza, M.C. Meletti-De-Oliveira, L. F. Marques-Santos, R.C. Maia, M.A.M. Capella, Multidrug resistance in tumour cells: characterisation of the multidrug resistant cell line K562-Lucena 1, An. Acad. Bras. Ci. 73 (2001) 57–69.
[21] Nathalia Daflon-Yunes, Flavio Eduardo Pinto-Silva, Raphael Silveira Vidal, Bruna Fortunato Novis, Tandressa Berguetti, Raphael Rodrigues Soares Lopes, Carla Polycarpo, Vivian M. Rumjanek, Characterization of a multidrug-resistant chronic myeloid leukemia cell line presenting multiple resistance mechanisms, Mol. Cell. Biochem. 383 (1-2) (2013) 123–135.
[22] J. Wang, J.J. Gildea, W. Yue, Aromatase overexpression induces malignant changes in estrogen receptor a negative MCF-10A cells, Oncogene 32 (2013) 5233–5240.
[23] M. Shozu, Y. Zhao, E.R. Simpson, Estrogen biosynthesis in THP1 cells is regulated by promoter switching of the aromatase (CYP19) gene, Endocrinology 138 (1997) 125–135.
[24] J.C. Moutford, C.M. Bruce, S.V. Hughes, M.T. Drayson, D. Webb, G. Brown, M. Hewison, Estrone potentiates myeloid cell differentiation: a role for 17 beta-hydroxysteroid dehydrogenase in modulating hemopoiesis, Exp. Hematol. 27 (1999) 451–460.
[25] C.M. Klinge, Estrogenic control of mitochondrial function, Redox Biol. 31 (2020), 101435.

[26] Matthew D. Hall, Misty D. Handley, Michael M. Gottesman, Is resistance useless? Multidrug resistance and collateral sensitivity, Trends Pharmacol. Sci. 30 (10) (2009) 546–556.
[27] Cátia Ramalhete, Silva Mulhovo, Hermann Lage, Maria-José Ferreira, Triterpenoids from Momordica balsamina with a Collateral Sensitivity Effect for Tackling Multidrug Resistance in Cancer Cells, Planta Med. 84 (18) (2018) 1372–1379.
[28] Adam I. Marcus, Ulf Peters, Shala L. Thomas, Sarah Garrett, Amelia Zelnak, Tarun M. Kapoor, Paraskevi Giannakakou, Mitotic kinesin inhibitors induce mitotic arrest and cell death in Taxol-resistant and -sensitive cancer cells, J. Biol. Chem. 280 (12) (2005) 11569–11577.
[29] Umar Faruk Mansoor, Angie R. Angeles, Chaoyang Dai, Liping Yang, Dilrukshi Vitharana, Andrea D. Basso, Kimberly Gray, Huadong Tang, Ming Liu, Lianzhu Liang, Omaira Allbritton, M. Arshad Siddiqui, Discovery of novel spiro 1,3,4-thiadiazolines as potent, orally bioavailable and brain penetrant KSP inhibitors, Bioorg. Med. Chem. 23 (10) (2015) 2424–2434.
[30] Amar Mohamed Ismail, Lionel L.A. In, Mohammad Tasyriq, Devi Rosmy Syamsir, Khalijah Awang, Ayda Hussein Omer Mustafa, Omer Fadul Idris, Imad Fadl-Elmula, Noor Hasima, Extra virgin olive oil potentiates the effects of aromatase inhibitors via glutathione depletion in estrogen receptor-positive human breast cancer (MCF-7) cells, Food Chem. Toxicol. 62 (2013) 817–824.
[31] Kristen M. Pluchino, Matthew D. Hall, Andrew S. Goldsborough, Richard Callaghan, Michael M. Gottesman, Collateral sensitivity as a strategy against cancer multidrug resistance, Drug Resist Updat 15 (1-2) (2012) 98–105.
[32] Eduardo J. Salustiano, Kelli M. da Costa, Leonardo Freire-de-Lima, Lucia Mendonça-Previato, José O. Previato, Inhibition of glycosphingolipid biosynthesis reverts multidrug resistance by differentially modulating ABC transporters in chronic myeloid leukemias, J. Biol. Chem. 295 (19) (2020) 6457–6471.
[33] D. Lorendeau, L. Dury, R. Nasr, A. Boumendjel, E. Teodori, M. Gutschow, P. Falson, A. Di Pietro, H. Baubichon-Cortay, MRP1-dependent collateral sensitivity of multidrug-resistat cancer cells: identifying selective modulators inducing cellular glutathione depletion, Curr. Med. Chem. 24 (2017) 1186–1213.
[34] Mari Miyajima, Hiroyuki Kusuhara, Kayo Takahashi, Tadayuki Takashima, Takamitsu Hosoya, Yasuyoshi Watanabe, Yuichi Sugiyama, Investigation of the effect of active efflux at the blood-brain barrier on the distribution of nonsteroidal aromatase inhibitors in the central nervous system, J. Pham. Sci. 102 (9) (2013) 3309–3319.
[35] C.A. Lipinski, F. Lombardo, B.W. Dominy, P.J. Feeney, Experimental and computational approaches to estimate solubility and permeability in drug discovery and development settings, Adv. Drug Deliv. Rev. 46 (2001) 3–26.
[36] J. Kelder, P.D.J. Grootenhuis, D.M. Bayada, L.P.C. Delbressine, J.-P.Ploemen.Polar Molecular Surface as a Dominating Determinant for Oral Absorption and Brain Penetration of Drugs, Pharm. Res.16 (1999) 1514–1519.
[37] H.Y. Yin, X.L. Lin, S.W. Li, L.X. Shao, N-heterocyclic carbene–palladium(II)- 1-methylimidazole complex catalyzed α-arylation reactions of tetralones with aryl chlorides and further transformation of the products, Org. Biomol. Chem. 13 (2015) 9012–9021.
[38] Stojan Stavber, Marjan Jereb, Marko Zupan, Direct α-Fluorination of Ketones Using N-F Reagents, Synthesis (17) (2002) 2609–2615, https://doi.org/10.1055/s-2002-35625.
[39] Y. Zhao, Y. Pan, H. Liu, Y. Yang, Z. Jiang, C.-H. Tan, Fluorinated Aromatic Ketones as Nucleophiles in the AsymmetricOrganocatalytic Formation of C-C and C-N Bonds: A Facile Route to theConstruction of Fluorinated Quaternary Stereogenic Centers, Chem. Eur. J. 17 (2011) 3571–3574.
[40] Stojan Stavber, Marjan Jereb, Marko Zupan, Solvent directing immediate fluorination of aromatic ketones using 1-fluoro-4-hydroxy-1,4-diazoniabicyclo [2.2.2]octane bis(tetrafluoroborate), Chem. Commun. (14) (2000) 1323–1324, https://doi.org/10.1039/b003488f.
[41] Zhiwei Jiao, Jason J. Beiger, Yushu Jin, Shaozhong Ge, Jianrong Steve Zhou, John F. Hartwig, Palladium-catalyzed enantioselective α-arylation of α-fluoroketones, J. Am. Chem. Soc. 138 (49) (2016) 15980–15986.
[42] D.M. Van der Kolk, E.G. de Vries, J.A. Koning, E. van den Berg, M. Muller, E. Vellenga, Activity and expression of the multidrug resistance proteins MRP1 and MRP2 in acute myeloid leukemia cells, tumor cell lines, and normal hematopoietic CD34+ peripheral blood cells, Clin. Cancer Res. 4 (7) (1998) 1727–1736.
[43] K. Yusa, T. Tsuruo, Reversal mechanism of multidrug resistance by verapamil: direct binding of verapamil to P-glycoprotein on specific sites and transport of verapamil outward across the plasma membrane of K562/ADM cells, Cancer Res. 49 (1989) 5002–5006.
[44] S.P. Cole, Multidrug resistance protein 1 (MRP1, ABCC1), a “multitasking” ATP-binding cassette (ABC) transporter, J. Biol. Chem. 289 (2014) 30880–30888.
[45] T. Sander, J. Freyss, M. von Korff, C. Rufener, DataWarrior: An Open-Source Program for Chemistry Aware Data Visualization And Analysis, J Chem Inf Model 55 (2015) 460–473.